ADVANCES IN MATERIALS SCIENCE, Vol. 19, No. 2 (60), June 2019

DOI: 10.2478/adms-2019-0010

M. H. Buszko [1,2], A. K. Krella[*1]

[1] *Institute of Fluid Flow Machinery, Polish Academy of Sciences, Fiszera 14, 80-231 Gdansk, Poland*
[2] *Gdansk University of Technology, Interdisciplinary Doctoral Studies, 11/12 Narutowicza, 80-233 Gdansk, Poland*
**akr@imp.gda.pl*

AN INFLUENCE OF FACTORS OF FLOW CONDITION, PARTICLE AND MATERIAL PROPERTIES ON SLURRY EROSION RESISTANCE

ABSTRACT

The degradation of materials due to slurry erosion is the serious problem which occurs in the power industries. The paper presents actual knowledge about an influence of individual factors connected with flow conditions, particles and material properties on the slurry erosion resistance. Among the factors connected with operating conditions, an influence of impact angle, and velocity of impact, particle concertation and liquid temperature have been described. In case of the factors connected with solid particle properties, an influence of the size, shape and hardness have been discussed. In the part devoted to the impact of material properties, due to different types of materials, the issues of resistance to erosion of slurries related to the properties of steel, ceramics and polymers are discussed separately. In the paper has been shown that a change of any of mentioned factors causes a change in the erosion rate due to the synergistic effects that accompany to slurry degradation.

Keywords: *erosion, slurry erosion, degradation, resistance, material properties*

INTRODUCTION

Slurry erosion is a process of material degradation due to the interaction with solid particles, called erodent, which are suspended in a flowing liquid. Due to multiple impacts of solid particles, material particles are removed from the exposed surface [1-3].Thus, the erosion process is depended on material properties, particles impacting the surface of material and flowing liquid. Fundamental examinations on slurry erosion were carried out since the 1960 s [4,5]. This phenomenon is especially dangerous in fluid-flow machinery, hydropower industry, and also in mining industry. The slurry erosion is a serious problem for the operation life, performance and reliability of the fluid-flow devices.

Erosion rate depends on many factors connected with fluid flow conditions (angle of impact, flow velocity, particles concentration, conditions of medium - liquid density, chemical activity and temperature), properties of target material (mechanical and endurance properties like toughness, fatigue, yield and ultimate strengths, work hardening, surface topography, surface morphology, microstructure, number and size of defects) and erodent

characteristics (size, shape, hardness, strength) [1,4,8,9]. The impact angle and material properties, including microstructure of a target, play the key role in the process of material removal [1,10-13], while impact velocity, particle concentration, size and hardness of solid particles are the significant parameters for erosion intensity and erosion rate. Along with an increase of these parameters erosion intensity increases [2,8,11,13-15]. Due to simultaneous action of the mentioned factors, degradation of material is a synergistic effect of these factors.

Until now investigations have shown that an increase of mechanical and endurance properties increase slurry erosion resistance. Therefore, in order to increase the resistance to erosion a surface treatment such as hardening or coating deposition are applied. Among several technology of coating deposition or surface layer modifications, laser treatment, cladding, plasma nitriding and thermal spraying methods are used [13,16,17]. The application of the coating like ceramic (e.g. chromium oxide, tungsten carbide), cermet (e.g. WC–Co) or metallic allows improving slurry erosion resistance by combining the beneficial properties of the core with wear resistance, hardness and heat resistance of the coating [13,18-24]. However, total elimination of erosion is impossible [6,7].

The aim of this paper is to present the key factors influencing slurry erosion rate associated with operating conditions, properties of solid particles (erodents) and target material. In order to better introduce properties associated with operating conditions and solid particles, each key parameter is described separately, while in case of target material properties, three categories of materials are presented: steels, ceramics and polymers.

FACTORS ASSOCIATED WITH OPERATING CONDITIONS

The most important factors related with fluid flow conditions are the impact angle, flow velocity and solid concentration. They influence the kinetic impact energy which is the main cause of material degradation. The first two mentioned factors, that is the impact angle and flow velocity influence impact energy of individual solid particle, while the third factor (particle condensation) influences cumulative impact energy. It should note that impact energy depends also on the size of erodent. The other fluid properties like density and viscosity play a lower role on erosion rate.

Impact angle

The impact angle is the main factor connected with operating conditions. This impact angle is defined as the angle between the direction of impact velocity of erodent (a solid particle) and target material. The impact angle has an influence on erosion rate of target material and discloses its brittleness [11]. Depending on hardness and plasticity of a target material, the maximum erosion rate occurs at different impact angle. In case of ductile materials, the maximum erosion rate usually occurs at 20 - 30° and further increase in an impact angle decreases the erosion rate. In case of stiff and brittle materials, the erosion rate increases with an increase of impingement angle, and the maximum erosion rate occurs at normal impact angle, i.e. at 90° (Fig.1). If an impact angle is close to zero, surface, especially of soft and ductile materials, is scratched by move of solid particle [1,8,11,26,27].

Investigations of Al-Bukhaiti et al. [1], who conducted tests on AISI 1017 steel with a content of 1.2 wt% Mn (200 HV) and chromium white cast iron with a content of 12.8 wt% Cr (686 HV) at impact angle of 15° to 90°, showed that impact angle has an effect on erosion

mechanism and erosion rate. In case of soft AISI 1017 steel, three degradation mechanisms were observed: (i) shallow plowing, and particle rolling occur for $\theta \leq 15^o$ -, (ii) deep ploughing and microcutting for $15^o < \theta < 70^o$ and (iii) for $75^o \leq \theta \leq 90^o$ - indentation with extruded material fatigue and wear dominate. In case of hard high-chromium white cast iron, only two types of degradation were observed: microcutting and plowing (for $\theta \leq 45\circ$) and indentation with lips of the ductile matrix, gross fracture as well as cracking of carbide phases and fatigue wear ($\theta > 45\circ$). The maximum erosion rate for soft AISI 1017 steel occurred at 45°. In case of hard high-Cr white cast iron, erosion rate increases with increasing the impact angle reaching its maximum value at 90^o – an angle typical for brittle materials [1,9,28,29]. In addition, the maximum erosion rate of high-Cr white cast iron, whose hardness is 3 times higher than 1017 steel, is over two times lower than that of AISI 1017 steel indicating on an increase of the slurry resistance with material hardness.

Arora et al. [3] investigated an effect of impact angles (30°, 60° and 90°) on erosion resistance of Zr44Ti11Cu10Ni10Be25 zirconium-based bulk metallic glass (BMG) with hardness of 6 GPa and CA6NM steel with a content of 13.5 wt% Cr hardness of 2.95 GPa. The erosion resistance of BMG was 2.6 and 1.6 times higher at the impact angle of 30° and 60°, respectively (Fig. 1). However, in case of the impact angle of 90°, the erosion rate for BMG was compared to CA6NM. Similar like in Ref. [1], the erosion mechanisms changes with an increase of impact angle. In case of BMG, erosion starts from microcutting at low impact angle, through shear bands and creation of ploughing marks elongated by particle movement at 30^o of impact angle and formation of shallow craters at 60^o to removal of material from steel surface. The major mechanism of material removal at 90^o impact angle is plastic deformation [3]. Thus, despite high hardness, BMG exhibit reasonable plasticity, which makes it more resistant to slurry erosion.

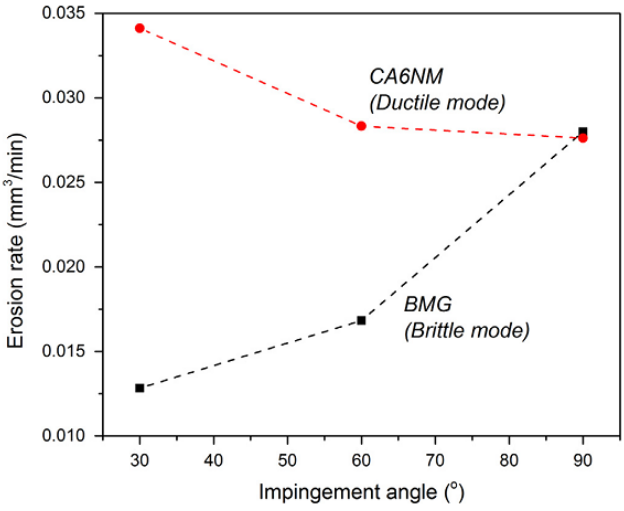

Fig. 1. The dependence of erosion rate on impact angle of zirconium-based bulk metallic glass (BMG) and CA6NM hydroturbine steel [3]

Investigations of an effect of impact angles (30°, 45°, 60°, 90°) on slurry erosion resistance for three stainless steels (304 and 316 steels with a content of 16-18 wt% Cr, and 420 steel a content of 13.6 wt% Cr) performed by Laguna-Camacho et al. [30] showed that 420 stainless steel with the highest hardness (200-240 HV) has the best erosion resistance. The maximum erosion rate occurred at 30° revealing domination of ductile behavior. In case of 316 (150 HV) and 304 (160 HV) steels, whose hardnesses are lower then 420 steel, have

approx. 5 -12 times higher erosion rate. 316 and 304 steels achieved maximum erosion rate at the impact angle of 60° indicating domination of brittle type of behavior, despite of low hardness. On the eroded surface of 316 and 304 steels were observed wear debris from abrasive particles and craters. At 90° of the impact angle, plastic deformation with pitting and cutting action occured. On the eroded surface of 420 steel, indentation scratches, plastic deformation with pitting and ploughing action were visible.

Grewal et al. [13] conducted tests on CA6NM steel with a content of 13.5 wt% Cr (296 HV) and three thermal sprayed coatings: Ni + 20% Al_2O_3 (563 HV), Ni + 40% Al_2O_3 (714 HV) and Ni + 60% Al_2O_3 (1141 HV) with impact angle of 30° and 90°. All coating have better slurry resistance than bare CA6NM steel. The best slurry erosion resistance had Ni+40%Al_2O_3 coating, which had also the highest fracture toughness. In case of CA6NM steel and Ni+20%Al_2O_3 coating, a ductile mode of erosion occurred, while in case of Ni+40%Al_2O_3 and Ni+60%Al_2O_3 coatings – a brittle mode of erosion. On the surface of eroded coatings, spalling (fracturing of Al_2O_3 splats) and cracking were observed.

Impact velocity

According to Ref. [31], the impact velocity has an effect on erosion rate and degradation mode due its influence on kinetic impact energy. In general, with increasing impact velocity increases erosion rate. At impact velocity lower than the critical / threshold velocity, solid particles slip on the target surface (due to friction force and low kinetic energy), so there is no cutting action. After approaching the threshold velocity, elastic deformation and fatigue degradation of material is observed. With further increase of impact velocity, degradation becomes more severe. The relationship between the erosion rate, E, and the impact velocity, *v*, has an exponential character, which is expressed as follow [2,32-36]:

$$E \propto v^{n_1} \tag{1}$$

where exponent n_1 depends on the material and fluid flow conditions and ranges from approx. 1 to 4 [2,11,32-37].

Lin and Shao [36] investigated three materials of different plasticity and hardness (pure aluminum with 28 HV, 1020 steel with a content of 0.2% Mn and 98 HV and high chromium cast iron with a content of 14.5% Cr and 703 HV) at various impact velocity in the range of 10 - 70 m/s and impact angle in the range of 15 – 90°. They obtained that the velocity exponent n_1 is in the range from 1.87 to 2.48. In addition, the impact angle influences the exponent n_1, which increased with increasing impact angle. However, higher erosion rate was notted at lower impact angles. This indicating on a ductile mode of fracture. Moreover, the velocity exponent n_1 decreased with an increase of target hardness that causes a decrease of materials ductility. Thus, both impact velocity and impact angle play the significant role in this type of erosion.

Levy et al. [38] tested hot-rolled 1018 steel (0.5% Mn) at three velocities (12, 21, 30 m/s). As an erodent was used coal-kerosene with concentration of 30 wt.%. Their investigations confirmed the connection of erosion rate with kinetic energy of solid particles and impact angle. The erosion rate increases exponentially with the impact velocity and the velocity exponent n_1 is in the range 1.62 – 2.12. The value of an exponent n_1 depends on impact angle: with increasing impact angle the power index decreases. Thus, they noticed an opposite correlation between a power index and impact angle than Lin and Shao [36]. This might be caused by much bigger concentration of solid particles in a slurry.

Oka et al. [2] tested several type of aluminum, copper, carbon steel and stainless steel using three types of solid particles and various impact angle (form 5° to 90°). According to their resutls, the power index n_1 is in the range of 2 - 3 and is related with impact angle, like in Refs [36] and [38]. On the other side, investigations of Bree et al. [32] of low-carbon steel showed that exponent n_1 is in the range of 3 – 4. Thus, taking into account only Refs [2,32,36,38], the velocity exponent n_1 can be in the range 1.87 – 4. According to Ref. [11], differences in the value of the power index resulted from different experimental conditions, fragmentation of solid particles and particles rotational energy.

Nguyen et al. [39] investigated erosion of stainless steel SUS-304 (18.2% Cr and 187 HB) at impact velocity of 10, 15, 20, 25 and 30 m/s. They confirmed that the erosion rate of stainless steel SUS304 increased with increasing impact velocity, but the erosion rate decreased to a critical value in the test time. According to their investigations, the velocity exponent n_1 is approx. 4 (4.09).

Particles concentration

The particles concentration is defined as volume (mass) of solid particles in the unit of volume (mass) of fluid. This factor can be also presented in the form of percentage of solid particle in a fluid volume (mass) or by parts per million unit (PPM). An effect of particle concentration is not simple and is related to the size of erodent [40].

Hawthorne [40] indicated that the erosion rate decreased with an increase of slurry concentration (5, 10, 15 wt.%). Similar correlation was noticed by Clark et al. [41]. According to Ref. [41], at the slurry concentrations of 0.86 vol.%, over 3 times higher material removal was observed than that at slurry concentrations of 12.6 vol.%. Clark et al. [41] assumed that with an increase in slurry concentration, a smaller amount of particles contacts the specimen surface that leads to a decrease in efficiency of material removal.

Grewal et al. [8] conducted tests on aluminum and cast iron. The variables were the impact angle (20° and 90°) and the slurry concentration (0.25 wt.% and 0.5 wt.%), while the impact velocity was constant and equaled of 25 m/s. Their investigation showed that with an increase of the slurry concentration increases volume loss (the erosion rate at 0.5 wt.% concentration results almost twice as compared to that at 0.25 wt.%). Similar result of an increase of erosion with an increase of the slurry concetration noticed Singh et al. [42], who examined an effect of slurry concentration on erosion of AISI 316 stainless steel, hard faced AISI 316 stainless steel with cobalt-based alloy and titanium based alloy. An increase of the slurry concentration from 40,000 ppm to 60,000 ppm caused an increase in the erosion rate.

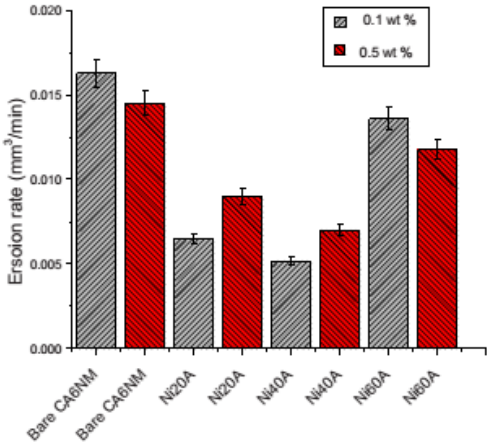

Fig. 2. Effect of slurry concentration [43]

Investigations of an effect of slurry concentration (0.1 wt.%, 0.5 wt.%) on erosion of Ni-Al_2O_3 based thermal spray coatings at impact velocity of 4 ± 0.5 m/s and impact angle of 90° performed by Grewal et al.'s [43] led to the following relationship between slurry erosion, E, and slurry concentration, C:

$$E = KC^{n_2} \tag{2}$$

where K is constant depending on the properties of material and erodent, and an exponent n_2 depends on the material properties. According to Ref. [43], the exponent n_2 was in the range from 0.9 to 1.3. Moreover, the erosion rate decreases with an increase of slurry concentration (Fig. 2). Similar like in Ref. [13], an increase of slurry resistance with increase in fracture toughness was noticed.

Similar effect of slurry concentration were observed in Ref. [40,44-46]. A decrease in erosion rate with an increase in slurry concentration can be related with the shielding effect of the rebounding solid particles. The erosion rate increases initially with increasing slurry concentration, but beyond a critical value of concentration, the interference between the incoming and rebounding solid particles plays an important role.

In slurry with a high concentration of solid particles, an increase of interaction between solid particles that attack and rebound from the eroded surface leads to loss of impact velocity and change the direction of impacting solid particles. The deviation of solid particles from their respective path may be so high that the attacking particles does not impinge on the eroded sample [47]. The final effect depends on the properties of a target material, but according to [47], an increase in the particle concentration causes a decrease of erosion rate up to limit value in most cases.

An increase in particle concentrations affects the Reynolds number and Stokes number. Bong et al. [48] investigated an effect of various solids concentration, C_v, (from 0.08 to 0.30 v/v) on mass transfer coefficient. The slurry consisted of aqueous NaOH solution and cationic ion-exchange resin with diameters of 0.6 – 0.7 mm and density of 1220 kg/m^3. The investigations showed that viscosity of the slurry increases with increasing solid particles concentration (Fig. 3a). Furthermore, the Reynolds number decreases as the concentration of solid particles increases (Fig. 3b). The obtained values of the Reynolds number showed that the slurry flow was in the turbulent region at a concentration of solid particles less than 0.2 v/v. However, with a concentration higher than 0.2 v/v, slurry flow reached the Re <10000, so was closer to the transition region.

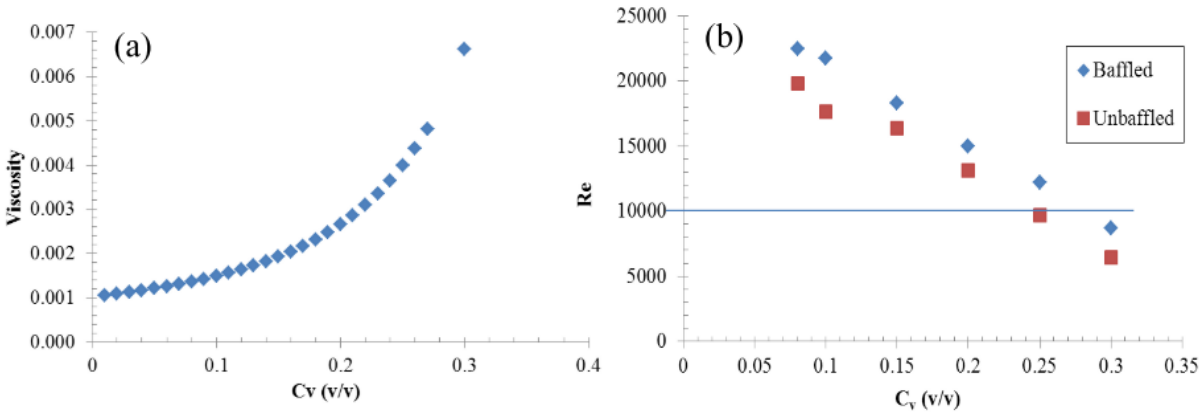

Fig. 3. Slurry concentration vs. (a) viscosity and (b) Reynolds number [48]

Shehadeh et al. [49] have investigated erosion-corrosion resistance of carbon steel. As erodent was used sand particle with concentration up to 9 g/l. The erosion-corrosion rate was influenced by the solid particles concentration and the Reynolds number (Fig. 4). The erosion rate increased with increasing solid particles concentration and the Reynolds number. In case of a solids concentration of 9g/l, the erosion rate increased fourfold with a change of laminar to turbulent flow.

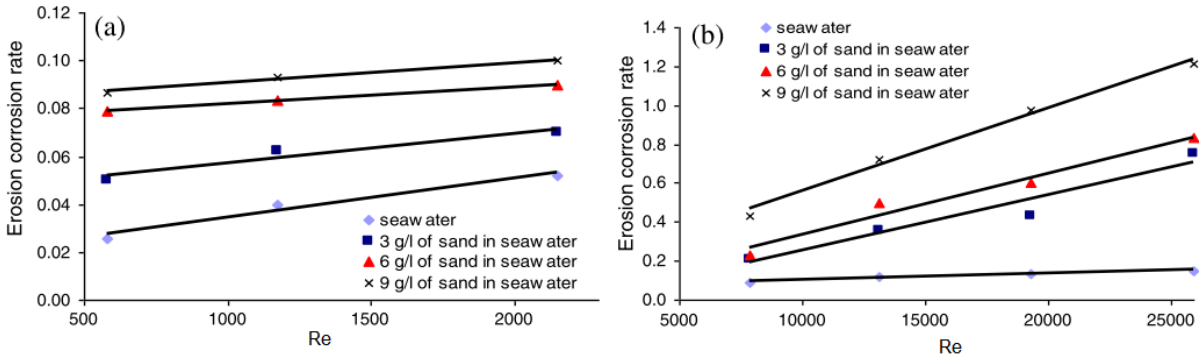

Fig. 4. The dependence erosion-corrosion rate on Reynolds number of carbon steel: (a) laminar flow, (b) turbulent flow [49]

To characterize the relationship between the solid particles and fluid movement, the Stokes number is used. According to Dabirian et al.'s investigations [50], the Stokes number increases with increasing particle size. Moreover, the Stokes number increases linearly with the increase in the concentration of solid particles (Fig. 5). In addition, Bartosik et al. [51] indicated that the solid concentration and the size of solid particles affect strongly on the 'particles–wall' shear stress. For example, the shear stresses increase from 1 Pa to 24 Pa as the particle size increases from 1 to 5 mm and the Reynolds number Re increases from Re = 72800 to Re = 189400 for the solid concentration of 20%. In the case of the solid concentration of 40%, the maximum shear stress increases to 110 Pa. According to Ref. [51], the concentration and the size of particles are more important than their density.

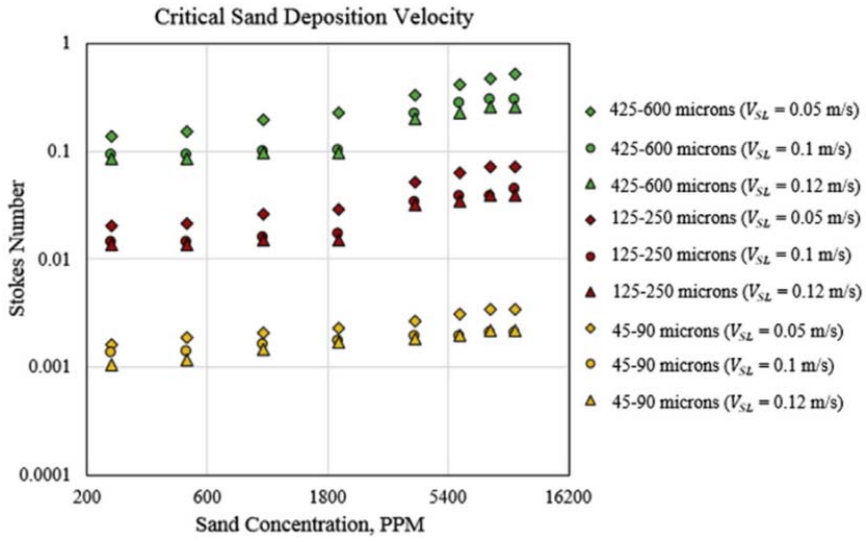

Fig. 5. Effect of slurry concentration on Stokes number [50]

In summarizing, an effect of slurry concentration depends on many parameters and is not completely described. In case of dilute slurries, erosion rate linearly increases with increase slurry concentration [8,52-55]. According to Refs [12,40,41,55], in case of higher concentration of slurry, slurry erosion may decrease with increase slurry concentration. On the other side, in Refs [29,45], no correlation between slurry concentration and slurry erosion were found. According to Ref. [56], an effect of slurry concentration on slurry erosion is compounded by particle collisions, particle rotation and sedimentation. Moreover, the Reynolds and Stokes number increased as the concentration of solid particles increased [48-50]. Thus, slurry concentration requires further investigations, because it plays a complex role in the slurry erosion process.

Temperature of liquid medium

Temperature is the next factor that affects the intensity of erosive wear. With increasing temperature the material ductility increases that results a change of degradation mechanism and an increase in erosion rate [57-60,65]. However, an influence of temperature is not as simple as it was mentioned above. Some investigations show a decrease in the erosion rate with an increase of temperature [58,59].

Sundararajan G. et al. [58] have conducted a literature review concerning the influence of temperature on erosive wear of metallic materials. Materials have been divided into three groups. The first group of materials are tungsten, 5Cr-0.5Mo, Alloy 800, 17-4PH, 410SS, Ti-6Al-4V, which show an initial decrease in the erosion rate and then increase in the erosion rate with increased temperature (Fig. 6a). In the second group of materials are 1100 aluminum (eroded at normal impact angle), 310SS (eroded at impact angle of 30°), 1018 steel, lead (eroded at impact angle of 20°) and Ta, which do not show a significant change in erosion rate, until the critical temperature was reached, and then started a rapid increase in the erosion rate (Fig. 6b). In the third group are materials like 2024 Al, 600, 12Cr-1Mo-V steel, carbon steel, lead (impact angle of 90°) and 2.25Cr-1Mo steel, which are characterized by a continuous increase in the erosion rate as the temperature increases (Fig. 6c).

Wang et al. [59] have investigated effect of elevated temperature on alumina ceramics. The tests were carried out at room temperature, 800°C, 1200°C and 1400°C at different impact angles (30°, 45°, 60°, 75° and 90°). As erodent were used SiC particles and corundum. The test results showed that the erosion rate of the tested material increases with increasing temperature. The rapid increase in mass losses starts after exceeding the temperature of 800°C. In addition, the maximum erosion rate was achieved at various impact angles. At room temperature and 800°C it was impact angle of 90°, while at 70° - 1200°C and at 1400°C - 90°. In addition, even at elevated temperatures, alumina ceramic showed brittle mechanism of erosion.

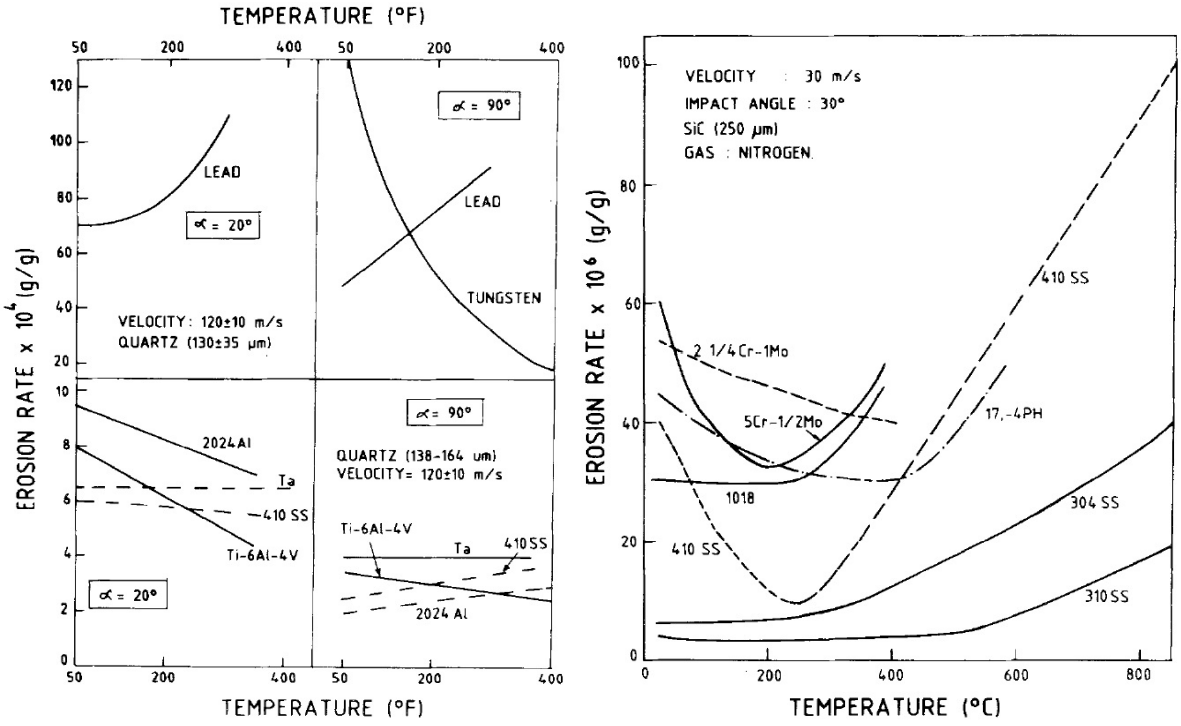

Fig. 6. Effect of temperature on erosion rate [58]

Sarlin et al. [60] investigated glass fibre reinforced vinylester composites (VE-FRP) at elevated temperature. Studies carried out at an impact velocity of 4.8 /s, solids concentration (quartz) of 15 wt% and an exposure time of 72 h showed a greater number of vapor cavities at a temperature of 95°C than 80°C. Moreover, on the suction side of the sample more vapor cavities appeared than on the pressure side samples and in the case of suction side degradation of the material was dominated more by cavitation. In addition, samples which were tested at 95°C were whiter compared to the samples tested at 80°, which can be explained by the hydrolytic degradation of the VE-FRP surface. The increase in temperature led to an increase in erosion rate. This is related to the softening of the target material (VE-FRP). Furthermore, AISI 316L steel was also tested at 80°C and 95°C as well as the same test conditions. Studies have shown a reduction in erosion rates as the temperature increased. Such results were influenced by the increase in the number of cavitation bubbles at higher temperatures, which interact with solid particles, reducing their kinetic energy.

FACTORS ASSOCIATED WITH SOLID PARTICLES (ERODENTS)

Removal of material from the surface during slurry erosion depends on mechanical properties, structure and geometric characteristics of erodent. Such parameters as the size, shape and hardness of solid particles significantly affect on the mechanism and rate of slurry erosion.

Particle size

Particle size is characterized by length and mass, or by diameter in case of spherical particles [37]. The size of erodent has an effect on the kinetic impact energy of a single particle. According to Refs [48,61-63], the relation between erosion rate and particle size present a power-law relationship in the form:

$$\text{erosion rate} \propto (\text{particle size})^{n}_{3} \tag{3}$$

where the value of exponent n_3 is in the range of 0.3-2.0. This difference in the value of the exponent is due to material properties, particle size and other operating conditions [63].

Sheldon and Finnie [64] investigated an effect of the size of silicon carbide particles (8.75 μm, 127 μm) on the erosion rate of ceramics, glass, graphite and steel at constant impact velocity of 152 m/s. With an increase in particle size from 8.75 μm to 127 μm the degradation mechanism changes from a ductile to a brittle mode. The peak of the maximum erosion rate moves from impact angle of about 20-40° to about 70-80° as shown in Fig. 7 [64,65]. The erosion rate of brittle materials like graphite and glass increased with an increase of particle size, while in case of hardened steel and annealed aluminum the erosion rate decreased. According to Ref. [64], a small diameter particle causes a cutting mechanism, while larger particles generate elastic deformation and fatigue wear of the target material.

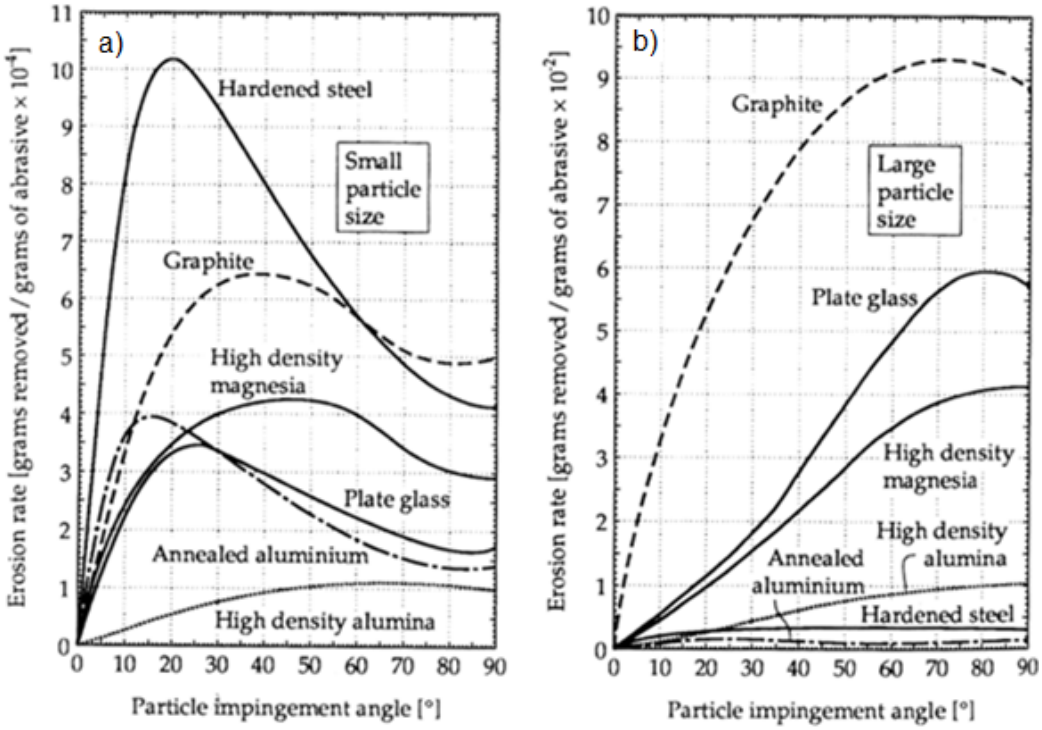

Fig. 7. Effect of abrasive particle size on erosive wear: a) tests carried out with particles of 8.75 μm in diameter, b) tests carried out with particles of 127 μm in diameter [65]

Lynn et al. [66] investigated an effect of the particle size on annealed copper and API P110 casing steel quenched and tempered. SiC particles with the diameter in range 20 – 500

μm were used as erodent and diesel oil was used as working liquid. As the particle size increases, the efficiency of the impact increases due to higher kinetic energy compared to the small solid particles. This results to increased erosion rate of tested materials.

Stack and Pungwiwat [61] conducted tests on stainless steel, iron, aluminum, teflon and alumina with erodents diameter in the size range of 250–1000 μm. As erodent were used alumina (1800 - 2000 HV) and silicon carbide (2100 - 2600 HV) particles. They noted that the correlation between the erosion rate and particle size was not monotonous, reaching a maximum value for the intermediate solid particle size (except for ceramic target surfaces). For alumina particles, the maximum of erosion rate appeared when particles diameter were within the range between 500 μm and 710 μm. For silicon carbide particles the main peak occurred for particles with the diameter of 710 μm. Their investigation confirmed that exponent n_3 is a function of target materials and properties of erodents.

Particle shape

Besides the size of solid particles, also their shape influences erosion rate. The erodent shape is described, in general, as angular, semiangular and rounded [67]. A particle shape plays an important role in value and distribution of contact stress in target material. In general, solid particulates with sharp irregular edges lead to increase the erosion rate, while solid particles with rounded edges causes less erosion rate [55,61,62,67-69].

In order to describe an effect of the shape, the aspect ratio, the roundness factor and circularity factor are used [70-73]:

- the roundness factor [68,70,72]: $\frac{P^2}{4 \cdot \pi \cdot A}$ (4)

where P is particle perimeter and A is projected area of the particle,

- the aspect ratio [68,70,72]: $\frac{W}{L}$ (5)

where W is particle width and L is particle length,

- the circularity [71,73]: $\frac{4 \cdot \pi \cdot A}{P^2}$ (6)

where P is overall perimeter of the projection of the particle and A is particle area.

Bahadur and Badruddin [68] investigated 18Ni (250) maraging steel. The roundness factor (Eq.4) and the aspect ratio (Eq.5) were used to characterized shape of erodent: SiC Al_2O and SiO_2. According to their investigations, the erosion intensity decreased with an increase of the aspect ratio (Eq.5) and increased with increasing the roundness factor (Eq.4). Similar like in Ref. [61], they noticed an increase in the erosion rates with an increase in the size for Al_2O_3 and SiC particles. However, in case of SiO_2 particles, an increase of their size caused a decrease in erosion rate.

Stachowiak [67] studied an effect of particle angularity and its influence on erosion intensity. For that reason, he introduced two parameters called "*spike parameter-linear fit*" (SP) and "*spike parameter-quadratic fit*" (SPQ). The SP is based on representation of the projected particle boundary by a set of triangles constructed at different scales, the SPQ is based on locating the center and the average radius of circle and represented by fitting

quadratic polynomial functions to protruding sections of particle boundary. His investigations showed that the relationship between the wear rate and the spike parameters (SP and SPQ) is almost linearly. The wear rate increases with increasing both spike parameters. Moreover, SPQ slightly better correlate with the wear rates comparing to SP. His results showed that both particle angularity parameters may be helpful in predicting and modeling of erosive and abrasive wear rates.

The influence of particle shape was also investigated by Al-Buchhaiti et al. [74]. As erodents, SiO_2 and SiC with various size and shape were used. Their investigations confirmed that erosion rate decreased with an increase of the aspect ratio (Eq.5) and circularity (Eq.6) for SiC. In case of SiO_2 particles, which were more rounded shape and closer to circularity than SiC particles, an opposite correlation was noted. The aspect ratio (Eq.5) decreased with the decrease of measured diameter for SiO_2 and increased with the decrease of diameter for SiC. Similar results associated with aspect ratio (Eq.5) were obtained by Bahadur and Badruddin [68].

Very important computational simulation (a micro-scale dynamic model - MSDM) were performed by Chen and Li [75], who investigated an effect of impact number of three basic type of particle shape: circle, triangle and square. In case of simple impact, triangular particle introduces the highest contact stress in target material, causes the highest material loss and cutting dominates in erosion mechanism. The circular particle caused only slightly bigger erosion than square particle. However, rotation of square particle increased erosion loss due to a decrease in contact surface and an increase in contact stress. The highest erosion was caused by square particle rotated 45°. In case of multi-impact (50 solid particles), the highest erosion loss was caused by triangular particles, similar like in simple impact. The erosion rate caused by square particles is considerably higher in comparison to that of circular particles.

Furthermore, Singh et al. [**76**] conducted image processing analysis (IPA) on SEM images to shape simulation of solid particles. Three types of erodents (iron-ore, bottom ash and fly ash) were used. The shape factors such as perimeter, circularity, roundness, sphericity, solidity of the solid particles were calculated from the scanning electron microscope images The highest value of the circularity shape factor showed the fly ash particles (0.75-0.95), while the lowest by the iron-ore particles (0.30-0.55). The same relationship occurred for the sphericity factor of solid particles. Furthermore, to analysis of surface smoothness was used grey value from the scanning electron microscope images. Fly ash particles were characterized by the highest surface smoothness, whereas bottom ash and iron-ore particles showed large irregularities (low surface smoothness).

Particle hardness

Particle hardness, similar to the particle shape, is a factor that significantly influences the erosion rate [77]. During the impact on target surface, the edges of the hard erodent remains sharp in opposition to soft solid particles, which round off even after small number of impacts [68]. The erosion rate increases when erodent have higher hardness than the target material. In case of soft particles, erosion occurs if the surface of the target material is characterized by low fracture toughness [3,37,78,79]. Thus, on slurry erosion rate, not only particle harness, but also hardness of target is essential. For that reason, the hardness ratio, which is preferably used, is expressed as follow [12,54,80,81]:

$$\frac{H_p}{H_t} \tag{7}$$

where H_p is hardness of solid particle and H_t is hardness of target material.

Lathabai et al. [77] conducted tests on Ce-TZP (stabilized tetragonal zirconia polycrystals) ceramics. As the erodent were used SiC, Al_2O_3 and SiO_2 with hardness of 26, 20, 12 HV, respectively. Their investigations confirmed very significant effect of hardness of solid particles on the slurry erosion resistance. The erosion rate increases as the particle hardness and the hardness ratio increases. Thus, the highest erosion rate was noted when SiC particles were used, and the lowest erosion rate was when in test SiO_2 were used.

Tsai et al. [82] conducted tests on ASTM A-53 carbon steel (133 HB), 316 (150 HB) and 304 (150 HB) stainless steel with two different erodents – SiC (9.5 HM) and coal (3.8 HM), which were suspended in kerosene. Their results showed 40–100 times higher erosion rate, when hard SiC particles were used than that of soft coal particles.

Desale et al. [12] investigated seven type of ductile materials (AA6063, copper, brass, mild steel – 0.5 wt% Mn, AISI 304L – 18.7 wt% Cr, AISI 316L – 17.3 wt% Cr, TBS – 13.5 wt% Cr) using three different solid particles – quartz (1100 HV), alumina (1800 HV) and SiC (2500 HV) with mean particle size of 550 μm in diameter and normal impact angle. Their investigations confirmed that erosion wear depends on the hardness ratio (Eq. 7). Desale et al. [12] noticed that there exists three regions of the hardness ratio, in which erosion rate of various target materials is comparable. The mass loss of target material increases, in general, with increasing hardness ratio.

FACTORS ASSOCIATED WITH TARGET MATERIALS

The erosive wear of ductile materials at a normal impact angle (90°) occurs mainly in the form of crater with extruded lips. However, at an oblique impact angle (20-30°), the material was removed by the microcutting and microploughing mechanism. In addition, brittle materials involves material removal mainly by crack formation (Fig. 8). Both erosion modes and mechanisms (ductile and brittle) may also occur together and depend on the properties of eroded material [65, 83, 84]. For the results obtained in the slurry tests, very important is to proper prepare the samples. Before each test, the surface of the samples should be ground on different gradations of emery paper and then polished. Polishing ends when a smooth mirror surface was reached.

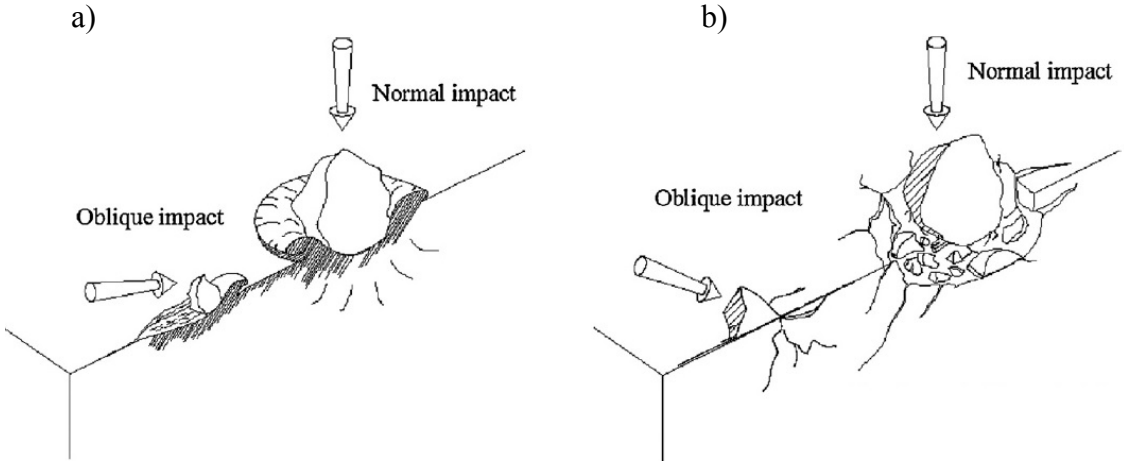

Fig. 8. Erosion mechanism of ductile materials (a) and brittle materials (b) at low and high impact angle [83]

This was important due to the removal of all surface contaminants and to remove scratches, which can be a source of an increase of erosion [17, 39,78]. In case of coated samples, grit blasting of the surface was also used to obtain a good adhesion between surface sample and coating [85, 86].

Generally, erosion rate and erosion resistance are associated with target material properties, such as hardness, toughness, fatigue, yield and ultimate strengths and elastic property. Due to the large differences in mechanical and strength properties between different types of materials, steels, ceramics and polymers will be described below separately.

Steels

Steels are characterized by good tensile strength, hardness and ductility, they eroded mainly in a ductile mode and the main erosion mechanism is scratching. Because steels are the most commonly used materials in technical devices where are exposed to the eroding environment, steels are the most investigated group of materials [17,18,37,87-89].

Levy [87] has performed extensive investigation of an effect of the microstructure of two ductile steels 1075 and 1020 on slurry erosion resistance. The 1075 steel in a spheroidized form showed better erosion resistant than that with coarse pearlite and fine pearlite microstructures, despite of the impact angle, the impact velocity and the slurry concertation [29]. Taking into account hardness of each steel state, the obtained result is surprising, because the best erosion resistance had the 1020 steel with the lowest hardness (10 HRB) and with increasing hardness the erosion resistance decreased. Performed cold-rolling (form 20% to 80%) of spheroidized 1075 steel results in an increase in the initial erosion rate. This erosion rate increase was connected with an increase of hardness from 242 HV_{1000} to 316 HV_{1000}, however, in case of 20% cold-rolling, an increase in the erosion rate is definitely lower that an increase of hardness. Levy's investigations [87] showed that besides hardness the microstructure of the tested steel plays the key role in the erosion resistance.

In case of 1020 steel, the important role in the erosion resistance play the carbide particle size and the spacing between these particles [87]. With increasing the distance between brittle carbide spheroids, the erosion resistance increases. However, if the particle spacing exceeds the limit value, the erosion rate decreases due to the low strength ferrite matrix. As a result, 1020 steel with hardness of 25 HRB had better erosion resistance than that of 30 HRB. Cracks and fracture of the cementite plates were observed on the surface of 1075 steel with pearlitic structure. In case of spheroidized structure of 1075 steel, cracks occur approx. 20 μm underneath the surface [87].

Gadhikar et al. [88] have investigated an effect of microstructure on the slurry resistance of 23-8-N steel (22.5 wt% Cr). The steel was examined in as-received state and after heat-treatment at 1050^{o}C, which was performed in order to solute carbides in the austenitic matrix. The heat treatment improves ductility and impact strength, but decreased yield strength, hardness and slightly ultimate tensile strength. Their investigations show that carbides are a barrier against the penetration of erodent into the tested material, but on the other side, they increase erosion rate by cracking and initiating decohesion of the matrix. After heat-treatment of 23-8-N steel erosion rate decreased of approximately 36% due to an essential improvement of steel ductility from 27.11% to 59% with slight decrease of hardness from 280 HV to 249 HV. The surface of heat-treated steel exhibits cutting marks and removal of material in the form of small pockets. In contrast, 23- 8-N steel without heat treatment showed large cavities and deep ploughs.

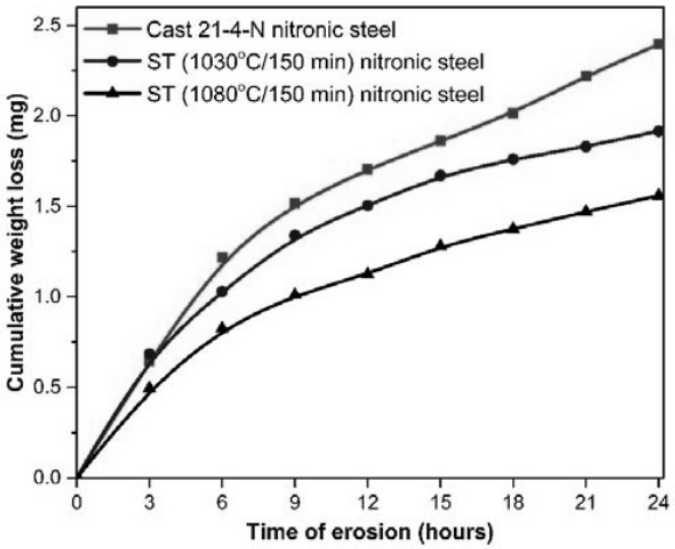

Fig. 9. The dependence of cumulative weight loss on time of tested materials [89]

An effect of carbide solution in 21-4-N nitronic steel (20.8 wt% Cr) on the slurry resistance was also investigated by Kumar et al. [89]. Heat treatment was carried out at 1030°C and 1080°C for 150 min in order to solute carbides in the austenitic matrix. An increase of temperature allowed to obtain more uniform structure and improve such mechanical properties like: ultimate tensile strength (UTS), ductility and impact energy, but hardness decreases. An increase of ductility from 14% to 25 % (heat treatment at 1030 °C) and to 37 % (heat treatment at 1080°C) caused an increase in the erosion resistance of about 20% and 34.8%, respectively, compared to cast 21-4-N nitronic steel (Fig. 9). Thus, ductility plays important role in increasing erosion resistance. Their investigation results are in agreement with those obtained by Levy's [87] and Gadhikar et al. [88]. The main erosion mechanism of cast 21-4-N nitronic steel was formation of craters and plough. The forms of degradation of material were smaller and less deep after solution annealing heat treatment.

An effect of modification of a surface layer on slurry erosion was investigated by Mann et al. [22] and Paul et al. [17]. Mann et al. [22] conducted tests on 13Cr–4Ni and T410 steels. 13Cr–4Ni steel has been subjected to several surface modification methods, in order to increase surface hardness. With an increase of surface hardness increases the erosion resistance. However, this increase is also related to the coating type. The best erosion resistance has T410 steel borided. The modified surface layer of T410 steel borided does not exhibit cracks or cavities comparing to 13Cr-4Ni steel borided, where cracks extending deep inside material.

Paul et al. [17] have investigated the erosion resistance (slurry and cavitation) of coatings produced by laser cladding such as: Metco-41C (Ni-Cr stainless steel powder, 225-250 $HV_{0.981N}$ and 17 % Cr), Colmonoy-5 (a NiCr-B-Si-C, 500-550 $HV_{0.981N}$ and 13.8 % Cr) and Stellite-6 (475-500 $HV_{0.981N}$ and 16.8 % Cr) on AISI 316L stainless steel (200 $HV_{0.981N}$). Hardness of all coatings was higher than that of substrate steel and independent on the number of layer claddings. Even though all coatings have better erosion resistance than the substrate stainless steel, an increase of the erosion resistance was not proportional to an increase in hardness. In case of test performed at impact angle of 30^o, the best slurry resistance has Metco-41C coating (225-250 HV), while in case of impact angle of 90^o, the best slurry resistance has Stellite-6 coating (475-500 HV). Additionally, both coatings (Metco-41C and Stellite-6) have similar resistance to cavitation erosion. They attributed an improvement of the erosion resistance to a combination of good toughness and work

hardening tendency, with the formation of fine dendrites structure and hard particulate constituents in soft matrices.

The simulations of erosion is very difficult due to many factors influencing simultaneously. Some of erosion models have been developed to take into account variable parameters that significantly affect the solid particle and eroded surface interaction [90]. Modern techniques for predicting the erosion process, such as Computational fluid dynamics (CFD) simulations, fuzzy model, are currently being used.

Wang el al. [91] has performed erosion test on throttle valve. The results obtained from Computational Fluid Dynamics (CFD) simulation were compared with the experimental results. A good correlation was obtained between the CDF analysis and the empirical test. Nevertheless, it was observed that the results were characterized by a divergent correlation with time. The reason for the discrepancy obtained was not to include the change in surface geometry as a function of slurry erosion in the CFD simulation.

Zhang et al. [92] conducted the experimental and CFD simulation tests on 30CrMo steel. As a erodent was used ceramic proppant with size of 0.300 mm - 0.425 mm, solids concentration of 7% vol., impact velocity from 5 m/s to 20 m/s as well as impact angles of 15° - 90°. The experimental studies indicated that the maximum erosion rate occurred at 30°. At low impact angles, the main mechanism of erosive wear were cutting and plowing, however, at high impact angles - the plastic deformation. In addition, the weight loss increased as the impact velocity increased and the power exponent, n, was approximately 2.2. The CFX simulation showed the erosive behavior of the exposed element. The biggest damage arose on the outer wall of elbow. In addition, the maximum erosion at the inner wall was located near to elbow outlet. The result obtained from the CDF simulation was consistent with the experimental results.

Singh et al. [93] have investigated erosion caused by bottom ash slurry in 90° elbow by the CFD analysis. To predict the slurry erosion was used discrete phase erosion wear model. Moreover, standard k–ε turbulence scheme for the slurry flow was used to particle tracking model. The results showed that erosion rate increased with the increase of the impact velocity. Furthermore, at low impact velocity, a distorted pattern appeared. However, at high impact velocities, a V-shaped pattern formed on the outer wall of 90° elbow. This was related with kinetic energy of the bottom ash slurry.

Hassan et al. [94] used a fuzzy logic model to predict erosive wear. Fuzzy logic is related to solving various problems that cover a wide range of applications and provides flexible solutions. Tests were carried out on 5127 steel, in which six parameters, such as impact angle, impact velocity, solids concentration, particle size, roundness factor and aspect ratio, were taken into account. With increasing impact velocity and particle size up to a limit value the erosion rate increases as well, but when the particle size exceeds the limit value, the erosion rate decreased. In addition, the erosion rate decreases with an increase in the concentration of solid particles, but increases with an increase in the aspect ratio. The results predicted by the fuzzy logic model were compared with the experimental results performed at impact angle of 30° and 90°, different particle sizes and impact velocities. The tests showed a good fit of the model values obtained, the maximum error was in the range from + 14% to -7%.

Hernik et al. [95] studied three types of materials: steel, aluminum and plasma coated steel with a layer of erosion. Iron oxide, quartz sand size 490, 1000, 1500 and 2000 μm and steel spheres with 100 μm diameter were used as erodes. Steel balls were used as a reference

standard and only for tests performed on a steel plate. The tests were carried out at an angle of 45°. The main goal was to experimentally determine the restitution rate and compare the experimental results with the results obtained from CFD simulations. The restitution coefficient was associated with the angle of reflection of particles from the eroded surface and the impact velocity of solid particles after impact and used for modeling erosion. The results obtained from the CFD analysis and experimentally were comparable. It was obtained that the highest values of the tangential restitution coefficient were obtained for aluminum, the lowest - for plasma steel with an anti-erosion layer

Ceramic

Ceramic materials are materials with ionic and covalent bonds, which cause strong bonding forces, and consist of non-metallic phases, mainly from oxides, nitrides, sulphides, carbides, phosphides. In general, ceramics possess high Young's modulus, hardness, melting point and low thermal expansion coefficient, but also have susceptibility to brittle fracture. Due to their high hardness and high temperature resistance, ceramic and cermet materials that contain ceramic and metallic phases are perspective coating materials for applications at high temperatures requiring resistance to erosion, e.g. steam turbines where there is a risk of drop erosion [18,96]. In cermet materials, the maximum erosion intensity occurs at intermediate angles. The erosion resistance depends on the phase composition of the coating and the test conditions [37, 97, 98].

Lathabai et al. [15] have investigated erosion resistance of several types of ceramic materials: yttria-stabilized tetragonal zirconia (3Y-TZP), alumina-fine, coarse-alumina, Al_2O_3-ZrO_2, Si_3Ni_4-SiC and soda-lime glass. The erosion results of ceramics were compared to 316L steel. Among all ceramics, only 3Y-TZP has better slurry resistance than 316L steel. However, no simple correlation between properties such as strength and / or hardness and mass loss was found. Lathabai et al. [15] have pointed that the reason is the microstructure of ceramics that has the central role in the erosion resistance. Ceramics eroded due to chipping out of lateral cracks, development of cracks along grain boundary, grain removal and in case of the soft phase of zirconia - plastic deformation [15].

Good erosion resistance of zirconia ceramic confirmed investigations of Fang et al. [29], who have tested four ceramic materials: partially stabilized zirconia PSZ, sialon 101, SiC and 85% Al_2O_3+15% SiO_2. PSZ zirconia has the lowest erosion rate independently from test conditions, sialon 101 characterizes better erosion resistance than SiC, but 85% alumina has the worse erosion resistance. The detailed microscopic study indicates that the degradation mechanisms of tested ceramics involve both brittle fracture and plastic deformation in the form of ripples, hills and valleys within the erosion craters. Preece and Macmillan [99] proposed to use the name of a "semi-brittle" degradation mode when a brittle and ductile mode occur together. In order to describe the erosion mechanism, the ratio of Hv / Kc (Hv is hardness, Kc is fracture toughness), called brittleness, was used. With increasing brittleness of ceramics increased the erosion rate. It was also shown that roughness did not play a significant role in the erosion rate, because with increasing of exposure time this parameter becomes insignificant.

Zhao et al. [28] conducted tests on ceramic coatings deposited by low pressure plasma-sprayed (LPPS) on pump impellers. The tests were performed using the jet and rotating types of slurry test rigs [5, 10]. The main test materials were: Cr_2O_3, Al_2O_3-TiO_3, ZrO_2-$8Y_2O_3$ as ceramic coatings, ZrO_2-Y_2O_3, Al_2O_3 , SiC, Si_3N_4 as bulk ceramics and SUS329J1 stainless steel as the reference material. The ceramic coatings have almost 2 times higher erosion resistance than SUS329J1. In particular Cr_2O_3 and Al_2O_3 coatings significantly improved the

slurry erosion resistance. As hardness of the tested material increases, the erosion rate decreases (Fig. 10). The correlation between the erosion rate, E, and the Vickers hardness, Hv, of ceramics is described in the following form [28]:

$$E = K(H_v)^{-n} \tag{8}$$

where K and n are constants.

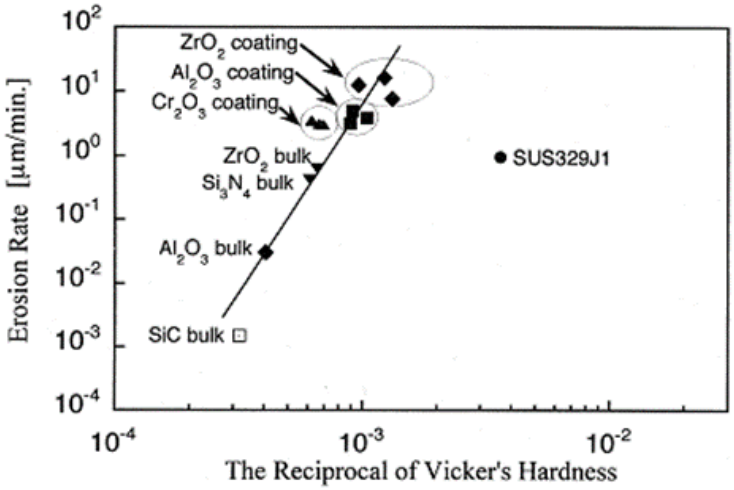

Fig. 10. The dependence of erosion rate on Vickers hardness of ceramic materials [28]

Investigation of an effect of the grain size of WC–10Co–4Cr powder used for coating deposition on AISI 304 stainless steel by means of HVOF spraying method was performed by Thakur et al. [16]. Two grain sizes were used: conventional grains (CWC) with the primary carbide size in the range between 2 to 4 μm and fine (near-nano) grains (NWC) with the primary carbide size in the range between 200 to 500 nm. Their investigations proved that using fine grains of powder for coating production increases the erosion resistance, mostly due to high hardness and fracture toughness. The coating produced from CWC eroded via cutting grooves, craters, lips, cracks, pull-out carbides and fractured WC grains. Similarly, cutting grooves, lips, WC extrusion and crack arrest were observed on the surface of the NWC coating.

Bhandari et al. [100] conducted tests on WC-10Co-4Cr cermet coating deposited on CF8M steel (17–21 % Cr) by means of detonation gun-spraying. Slurry tests decrease surface roughness (Ra parameter) of both coating and bare steel, but the degree of this decrease was different for cermet coating and steel, and depended on the test conditions. A reduction in surface roughness of eroded steel was in the range from 15.4 to 57.7 %, while in case of the coating, it was in the range from 14.5 to 17.3 %. The lower decrease of Ra parameter of WC-10Co-4Cr coating was caused by its high hardness. Hardness of steel, which initially was approx. 6 times lower than that of coating, increased from 190 ± 20 HV to 260 ± 20 HV during the slurry tests. Degradation of CF8M steel occurred due to cutting, plowing, formation of craters, deep cavities and lips. WC-10Co-4Cr coating surface eroded mainly in a brittle mode: cutting and removal of coating particles.

Polymers

The polymers are wide group of synthetic chemical substances with density in range from 0.15 to 3.8 g/cm^3, but majority of them have density slightly greater than 1 g/cm^3. Therefore, interest in this group of light materials is growing, especially in aviation [101]. Most of polymers are very sensitive on temperature, therefore their application is limited. Due to an effect of temperature, polymeric materials are divided into thermoplastic and thermosets materials. In contrast to the thermoplastic materials, the thermosets materials show a brittle mode of fracture [102]. Although erosion resistance of polymers is generally inferior to steels, but in some cases they exhibit better resistance, e.g. polyurethane with nano-SiC particles has better erosion resistance than 16Cr-5Ni martensitic stainless [86]. On the other side, elastomer coatings, which are very soft materials, have poor erosion resistance in high velocity jet erosion test and therefore, they are not recommended for hydropower turbine elements [37]. According to Ref. [12], the erosion resistance of usually used polymers is as follows: nylon < ploymethylmethacrystalate < polycarbonate fluorocarbon< polyurethane.

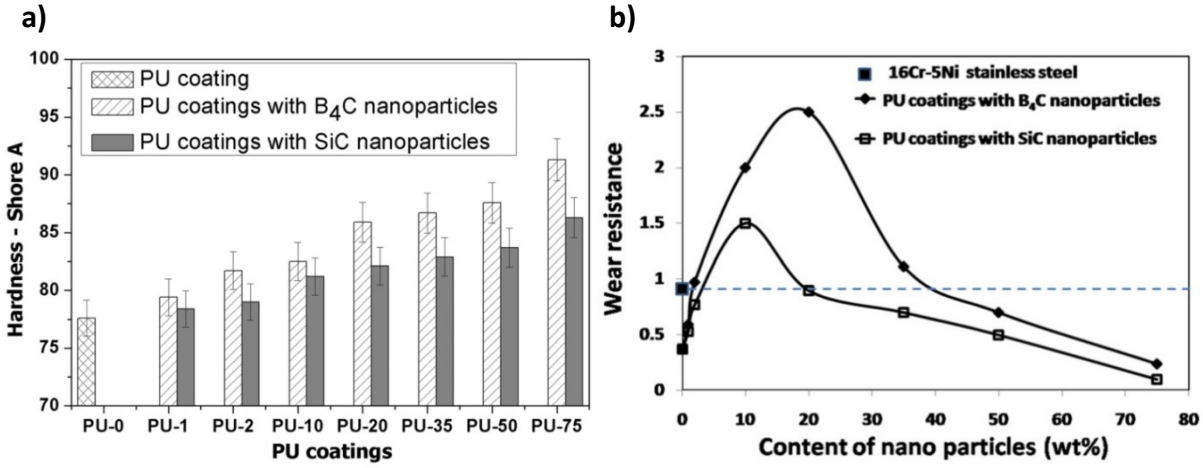

Fig. 11. The dependence of Shore hardness on PU coatings (a) and relationship between wear resistance and content of B4C / SiC nanopraticles (b) [85]

Syamsundar et al. [86] have investigated the erosion behavior of five polyurethane (PU) coatings, which varied concentration of a hardening agent (nano-B_4C and nano-SiC powder). The PU coatings were deposited on the 16Cr-5Ni martensitic stainless steel. Their investigations showed that addition of B_4C or SiC nanoparticles to epoxy resin increase hardness and erosion resistance of the coatings in comparison to PU coating without nanoparticles and 16Cr-5Ni stainless steel. This is associated with an increase in hardness of the coatings after the addition of nanoparticles. In addition, better erosion resistance have the coatings with B_4C nanopartlices, due to higher hardness than coatings with SiC nanopartlices (Fig. 11a). Syamsundar et al. [86] noticed that the optimal level of nanoparticles added to the PU coating was 20 wt.% for B_4C nanopartlices and 10 wt.% for SiC nanopartlices (Fig. 11b). This may be due to the fact of nonhomogeneous dispersion of B_4C and SiC nanoparticles on polyurethane matrix that leads to earlier degradation of the surface by cracks and interfacial defects. The improvement of wear resistance was 50 % by using PU coatings with 10 wt.% of SiC nanoparticles, and 150 % with 20 wt.% of B_4C compared to uncoated 16Cr-5Ni stainless steel (Fig. 11b). Coating's roughness increased with the increase in the content of B_4C / SiC nanoparticles. In addition, surface roughness of the coatings with SiC nanopartices is

generally higher than that of B_4C nanopartices. The main erosion mechanism of 20 wt.% B_4C nanoparticle-reinforced PU coating was formation of groove and craters. The coating with 10 wt.% SiC nanoparticles was eroded due to hole formation (after removal/pullout of the SiC nanoparticle), craters and microcutting. On the pure PU coating occurred cluster of craters, primary and secondary erosion sites. Furthuremore, the uncoated 16Cr-5Ni stainless steel exibited formation of craters, lips and plowing

Zahavi et al. [103] have investigated three polymeric coatings: an elastomeric MIL-C-83231 polyurethane, hard MIL-C-83286 polyurethane and an elastomeric AF-C-VBW-15-15 fluorocarbon applied on an E glass-epoxy laminate substrate. The impact angle can be varied from 15° to 90° as well as slurry concentration of 200 g, 400 g and 600 g. The erosion rate increase with increasing slurry concentration and decreasing impact angles for all coatings. The polymeric coatings showed typical ductile behavior – the maximum mass loss occurs at impact angle of 30° and minimum at 90°. The impact angle and erosion rate influence surface roughness. The hard MIL-C-83286 polyurethane coating showed the maximum roughness at 30°-45°, for the elastomeric AF-C-VBW-15-15 fluorocarbon coating at 30° and for elastomeric MIL-C-83231 polyurethane at 15°. On the coatings surface occurred degradation in few steps: microcracks, propagation of microcracks and intersection, separation (detachment) of pieces of coatings and local removal of material.

Lima et al. [104] conducted tests on Polyamide 12 (PA12), Poly-ether-ether-ketone (PEEK) and Polyetherimide (PEI) coatings deposited on AISI 1020 (low-carbon steel) by low-pressure flame spray technology. The polymeric coatings had adhesion value in range from 10 MPa (PEI) to 12 MPa (PEEK). The highest hardness has PEI coating (90 Shore D) and the lowest - PEEK coating (82 Shore D). The erosion rate was lowest at impact angle of 90° for PA12 and PEEK coatings. On the coatings surface, plowing and fatigue tearing were visible. The PEI coating achieve similar mass loss for 30° and 90° of impact angle, but worse performance than PEEK and PA12 at 90°. The PEI coating surface presented cracks, pores and holes.

SUMMARY

In the paper, the most essential factors affecting slurry erosion rate are presented. The degradation of materials depends on fluid flow conditions such as flow velocity, impact angle, particles concentration, as well as solid particles characteristic like size, shape and hardness, and properties of target material, that is hardness, toughness and microstructure. Due to simultaneous action of these factors, a synergistic effect occurs in material degradation and erosion rate, that is seen in the exponential relationships between erosion rate, E, and flow velocity, *v*, slurry concentration, C, and particle size, D:

$$E \propto v^{n_1}, C^{n_2}, \mathrm{D}^{n_3} \tag{9}$$

An exponent n_1 of flow velocity is in the range 1.87 – 4, an exponent n_2 of solid particle concentration is in the range from 0.9 to 1.3, and an exponent n_3 of the solid particle size is in the range of 0.3-2.0.

En effect of the impact angle depends on material stiffness. Ductile materials achieve the maximum erosion rate at impact angle in range from 20° to 30°, while brittle materials at normal or close to normal impact angle. An effect of particle concentration is much more complicated, because it depends also on the slurry concentration. In case of dilute slurries, an

increase of particle concentration increases erosion rate. However, if slurry concentration exceeds the limit value, an increase of particle concentration decrease erosion rate. This is due to an increase number of collisions between particles before they reach the target surface leading to decrease of impact velocity. Consequently the kinetic energy of the erodents decreases causing lower material loss from the target surface. In some investigations, no correlation between slurry concentration and slurry erosion were found and an effect of slurry concentration on slurry erosion is also compounded by particle rotation and sedimentation. Because slurry concentration play important role in erosion process and is not wholly understood, it requires further depth investigations.

The size and shape of solid particles play also crucial role in material degradation and slurry erosion rate. In general, big and angular particles cause more intensive mass loss and erosion rate. Such solid particles generate sharp indents and narrow cutting grooves in target material. In case of rounded particles, solid particles produce round craters and smooth grooves. Additionally, with increasing hardness of erodent increases erosion rate.

The erosion resistance of steels depends strongly on material hardness, and also on structure, that is the grain size and the number and size of defects. Thermal treatment, which influence hardness and ductility by changing the structure allows to improve the slurry erosion. Ceramics, which possess high hardness and strength characterize good erosion resistance, although they possess high susceptibility to brittle fracture. In general, with increasing material brittleness, the erosion rate increases as well. Polymers, whose hardness is much lower than steels and ceramics, have lower erosion resistance. However, addition of some nanoparticles, which change polymer structure and increase hardness, increase also the erosion resistance. In general, with an increase of hardness, fracture toughness and ductility the erosion resistance increases as well. Due to an effect of hardness on the erosion resistance, the main method of protecting the materials surface against slurry erosion is the deposition of hard coatings, such as WC-based coatings, Ni-based coatings and also polyurethane coatings containing nanoparticles such as B_4C or SiC. Additives to the coatings in the form of nanoparticles or / and carbon nanotubes leads to increase their microhardness and fracture toughness as well as a decrease in roughness and porosity.

REFERENCES

1. Al-Bukhaiti M. A., Ahmed S. M., Badran F. M. F., Emara K. M., Effect of impingement angle on slurry erosion behaviour and mechanisms of 1017 steel and high-chromium white cast iron. Wear, 262 (2007) 1187–1198.
2. Oka Y. I., Okamura K., Yoshida T., Practical estimation of erosion damage caused by solid particle impact: Part 1: Effects of impact parameters on a predictive equation. Wear, 259 (2005) 95–101.
3. Arora H. S., Grewal H. S., Singh H., Mukherjee S., Zirconium based bulk metallic glass-Better resistance to slurry erosion compared to hydroturbine steel. Wear, 307 (2013) 28–34.
4. Finnie I., Erosion of surfaces by solid particles. Wear 3 (1960) 87–103.
5. Bitter J.G.A., A study of erosion phenomena, part I. Wear 6 (1963) 5-21.
6. Zbrowski A., Mizak W., Analiza systemów wykorzystywanych w badaniach uderzeniowego zużycia erozyjnego. Problemy eksploatacji, 3 (2011) 235–250, (in Polish)

7. Sinha S.L., Dewangan S.K., Sharma A., A review on particulate slurry erosive wear of industrial materials: In context with pipeline transportation of mineral−slurry. Particulate Science and Technology, 35 (2017) 103-118.
8. Grewal H. S., Agrawal A., Singh H., Design and development of high-velocity slurry erosion test rig using CFD. Journal of Materials Engineering and Performance, 22 (2013) 152–161.
9. Finnie I., Some reflections on the past and future of erosion. Wear 186-187 (1995) 1-10.
10. Buszko M.H., Krella A.K., Slurry erosion – design of test devices. Advances in Materials Science 17 (2017) 5-17.
11. Shitole P. P., Gawande S. H., Desale G. R., Nandre B. D., Effect of impacting particle kinetic energy on slurry erosion wear. Journal of Bio-and Tribo-Corrosion 1 (2015) 1–9.
12. Desale G.R., Gandhi B.K., Jain S.C., Slurry erosion of ductile materials under normal impact condition. Wear, 264 (2008) 322-330.
13. Grewal H. S., Agrawal A., Singh H., Shollock B. A., Slurry erosion performance of Ni-Al_2O_3 based thermal-sprayed coatings: Effect of angle of impingement. Journal of Thermal Spray Technology, 23 (2014) 389–401.
14. Grewal H. S., Agrawal A., Singh H., Slurry erosion mechanism of hydroturbine steel: Effect of operating parameters. Tribolology Letters, 52 (2013) 287–303.
15. Lathabai S., Pender D. C., Microstructural influence in slurry erosion of ceramics. Wear, 189 (1995) 122–135.
16. Thakur L., Arora N., A comparative study on slurry and dry erosion behaviour of HVOF sprayed WC-CoCr coatings. Wear, 303 (2013).
17. Paul C.P., Gandhi B.K., Bhargava P., Dwivedi D.K., Kukreja L.M., Cobalt-Free Laser Cladding on AISI Type 316L Stainless Steel for improved cavitation and slurry erosion Wear Behavior. Journal of Materials Engineering and Performance, 23 (2014) 4463-4471.
18. Hejwowski T., Nowoczesne powłoki nakładane cieplnie odporne na zużycie ścierne i erozyjne. Politechnika Lubelska, Lublin, 2013, (in Polish).
19. Clark H. M., Hawthorne H. M., Xie Y., Wear rates and specific energies of some ceramic, cermet and metallic coatings determined in the Coriolis erosion tester. Wear, 233–235 (1999) 319–327.
20. Santa J.F., Baena J.C., Toro A., Slurry erosion of thermal spray coatings and stainless steels for hydraulic machinery. Wear 263 (2007) 258–264.
21. Santa J.F., Espitia L.A., Blanco J.A., Romo S.A., Toro A., Slurry and cavitation erosion resistance of thermal spray coatings. Wear, 267 (2009) 160–167.
22. Mann B.S., High-energy particle impact wear resistance of hard coatings and their application in hydroturbines. Wear, 237 (2000) 140–146.
23. Mann B.S., Arya V., Abrasive and erosive wear characteristics of plasma nitriding and HVOF coatings: Their application in hydro turbines. Wear, 249 (2001) 354-360.
24. Romo S.A., Santa J.F., Giraldo J.E., Toro A., Cavitation and high-velocity slurry erosion resistance of welded Stellite 6 alloy. Tribology International, 47 (2012) 16-24.
25. Hutchings I.M., Tribology: Friction and Wear of Engineering Materials. Edward Arnold, London, 1992.
26. Thakur P.A., Khairnar H.S., Deore E.R., More S.R., Development of slurry jet erosion tester to simulate the erosion wear due to solid-liquid mixture. International Journal of Novel Research in Engineering and Science, 2 (2015) 14-20.

27. Saleh B., Ahmed S.M., Slurry erosion-corrosion of carburized AISI 5117 steel. Tribolology Letters, 51 (2013) 135-142.

28. Zhao H.X., Goto H., Matsumura M., Takahashi T., Yamamoto M., Slurry erosion properties of ceramic coatings. Wear, 233-235 (1999) 608-614.

29. Fang Q., Xu H., Sidky P.S., Hocking M.G., Erosion of ceramic materials by a sand/water slurry jet. Wear, 224 (1999) 183-193.

30. Laguna-Camacho J.R., Marquina-Chávez A., Méndez-Méndez J.V., Vite-Torres M., Gallardo-Hernández E.A., Solid particle erosion of AISI 304, 316 and 420 stainless steels. Wear, 301 (2013) 398-405.

31. Basha S. S., Periasamy V. M., Kamaraj M., Slurry erosion resistance of laser-modified 16Cr – 5Ni stainless steel. International Journal of ChemTech Research, 6 (2014) 691–704.

32. de Bree S., Rosenbrand W., de Gee A., On the erosion resistance in water-sand mixtures of steels for application in slurry pipelines. Proc. 8th Int. Conf. Hydraulic Transport of Solids in Pipes, BHRA Fluid Engineering, Johannesburg, 1982, Paper C3.

33. Fuyan L., Hesheng S., The effect of impingement angle on slurry erosion. Wear, 141 (1991) 279-289.

34. Gandhi B.K., Singh S.N., Seshadri V., Study of the parametric dependence of erosion wear for the parallel flow of solid-liquid mixtures. Tribology International, 32 (1999) 275-282.

35. Gupta R., Singh S. N., Sehadri V., Prediction of uneven wear in a slurry pipeline on the basis of measurements in a pot tester. Wear, 184 (1995) 169–178.

36. Lin F. Y., Shao H. S., Effect of impact velocity on slurry erosion and a new design of a slurry erosion tester. Wear, 143 (1991) 231–240.

37. Thapa B., Sand erosion in hydraulic machinery. PhD Thesis, Norwegian University of Science and Technology (NTNU), 2004.

38. Levy A.V., Yau P., Erosion of steels in liquid slurries. Wear, 98 (1984) 163-182.

39. Nguyen Q. B. Lim C.Y.H., Nguyen V.B., Wan Y.M., Nai B., Zhang Y.W., Gupta M., Slurry erosion characteristics and erosion mechanisms of stainless steel. Tribology International, 79 (2014) 1–7.

40. Hawthorne H.M., Some Coriolis slurry erosion test developments. Tribology International, 35 (2002) 625-630.

41. Clark H.M., Tuzson J., Wong K.K., Measurements of specific energies for erosive wear using a Coriolis erosion tester. Wear 241 (2000) 1-9.

42. Singh G., Virdi R. L., Goyal K., Experimental investigation of slurry erosion behaviour of hard faced AISI 316L Stainless Steel. Universal Journal of Mechanical Engineering 3 (2015) 52-56.

43. Grewal H. S., Arora H. S., Agrawal A., Singh H., Mukherjee S., Slurry erosion of thermal spray coatings: Effect of sand concentration. Procedia Engineering 68 (2013) 484–490.

44. Turenne S., Fiset M., Masounave J., The effect of sand concentration on the erosion of materials by a slurry jet. Wear, 133 (1989) 95-106.

45. Prasad B.K., Jha A.K., Modi O.P., Yegneswaran A.H., Effect of sand concentration in the medium and travel distance and speed on the slurry wear response of a zinc-based alloy alumina particle composite. Tribolology Letters, 17 (2004) 301-304.

46. Burnett A.J., De Silva S.R., Reed A.R., Comparisons between “sand blast” and “centripetal effect accelerator” type erosion testers. Wear, 186-187 (1995) 168-178.

47. Kleis. I, Kulu P., Solid Particle Erosion. [In] Influence of Particle Concentration. Springer-Verlag London Limited, 2008, 24-27.
48. Bong E.Y., Parthasarathy R., Wu J., Eshtiaghi N., Effect of baffles on solid-liquid mass transfer coefficient in high solid concentration mixing. Chemeca 2012: Quality of life through chemical engineering, Wellington, New Zealand, 2012, 1870- 1880.
49. Shehadeh M., Anany M., Saqr K.M., Hassan I., Experimental investigation of erosion corrosion phenomena in a steel fitting due to plain and slurry seawater flow. International Journal of Mechanical and Materials Engineering, 9 (2014) 1-9.
50. Dabirian R., Mohan R., Shoham O., Kouba G., Critical sand deposition velocity for gas liquid stratified flow in horizontal pipes. Journal of Natural Gas Science and Engineering, 33 (2016) 527-536.
51. Bartosik A., Influence of coarse-dispersive solid phase on the 'particles–wall' shear stress in turbulent slurry flow with high solid concentration. The Archive of Mechanical Engineering, 57 (2010) 45-68.
52. Bjordal M., Bardal E., Rogne T., Eggen T.G., Combined erosion and corrosion of thermal sprayed WC and CrC coatings. Surface and Coatings Technology 70 (1995) 215-220.
53. Padhy M.K., Saini R.P., Effect of size and concentration of silt particles on erosion of Pelton turbine buckets. Energy 34 (2009) 1477-1483.
54. Elkholy A., Prediction of abrasion wear for slurry pump materials. Wear, 84 (1983) 39-49.
55. Lindgren M., Perolainen J., Slurry pot investigation of the influence of erodent characteristics on the erosion resistance of austenitic and duplex stainless steel grades. Wear, 319 (2014) 38-48.
56. Zitoun K., Sastry S., Guezennec Y., Investigation of three dimensional interstitial velocity, solids motion, and orientation in solid–liquid flow using particle tracking velocimetry. International Journal of Multiphase Flow, 27 (2001) 1397-1414.
57. Yang J.-Z., Fang M.-H., Zhao-Hui Huang Z.-H., Hu X.-Z., Liu Y.-G., Sun H.-R., Huang J.-T., Li X.-Ch., Solid particle impact erosion of alumina-based refractories at elevated temperatures. Journal of the European Ceramic Society 32 (2012) 283–289.
58. Sundararajan G., Roy M., Solid particle erosion behavior of metallic materials at room and elevated temperatures. Tribology International, 30 (1997) 339-359.
59. Wang X., Fang M., Zhang L.-C., Ding H., Liu Y.-G., Huang Z., Huang S., Yang J., Solid particle erosion of alumina ceramics at elevated temperature. Materials Chemistry and Physics, 139 (2013) 765-769.
60. Sarlin E., Lindgren M., Suihkonen R., Siljander S., Kakkonen M., Vuorinen J., High-temperature slurry erosion of vinylester matrix composites – The effect of test parameters. Wear, 328-329 (2015) 488-497.
61. Stack M.M., Pungwiwat N., Slurry erosion of metallics, polymers, and ceramics: particle size effects. Materials Science and Technology 15 (1999) 337-344.
62. Gandhi B.K., Borse S.V., Nominal particle size of multi-sized particulate slurries for evaluation of erosion wear and effect of fine particles. Wear, 257 (2004) 73-79.
63. Desale G.R., Gandhi B.K., Jain S.C., Particle size effects on the slurry erosion of aluminium alloy (AA 6063). Wear, 266 (2009) 1066-1071.
64. Sheldon G.L., Finnie I., On the ductile behaviour of nominally brittle materials during erosive cutting. Journal of Engineering for Industry, 88 (1966) 387-392.

65. Stachowiak G.W., Batchelor A.W., Engineering Tribology (fourth edition). [In] Abrasive, Erosive and Cavitation Wear. Elsevier Butterworth-Heinemann, 2014, 525-576.

66. Lynn R.S., Wong K.K., Clark H.M., On the particle size effect in slurry erosion. Wear, 149 (1991) 55-71.

67. Stachowiak G.W., Particle angularity and its relationship to abrasive and erosive wear. Wear, 241 (2000) 214-219.

68. Bahadur S., Badruddin R., Erodent particle characterization and the effect of particle size and shape on erosion. Wear, 138 (1990) 189-208.

69. Desale G.R., Gandhi B.K., Jain S.C., Effect of physical properties of solid particle on erosion wear of ductile materials. Porc. of World Tribology Congress III, Washington, D.C., USA, 2005, 149-150.

70. Raadnui S., Wear particle analysis - Utilization of quantitative computer image analysis: A review. Tribology International, 38 (2005) 871-878.

71. Bouwman A.M., Bosma J.C., Vonk P., Wesselingh J. (Hans) A., Frijlink H.W., Which shape factor(s) best describe granules?. Powder Technology, 146 (2004) 66–72.

72. Roylance B.J., Raadnui S., The morphological attributes identifying wear mechanisms of wear particles their role in identifyinf wear mechanisms. Wear 175 (1994) 115-121.

73. Cox E.P., A method of assigning numerical and percentage values to the degree of roundnedd of sand grains. Journal of Palentology, 1 (1927) 179-183.

74. Al-Bukhaiti M.A., Abouel-Kasem A., Emara K.M., Ahmed S.M., Particle shape and size effects on slurry erosion of AISI 5117 steels. Journal of Tribology, 138 (2016).

75. Chen Q., Li D.Y., Computer simulation of solid particle erosion. Wear, 254 (2003) 203-210.

76. Singh J., Kumar S., Mohapatra S.K, Kumar S., Shape simulation of solid particles by digital interpretations of scanning electron micrographs using IPA technique. Materials Today: Proceedings, 5 (2018) 17786–17791.

77. Lathabai S., Effect of grain size on the slurry erosive wear of Ce-TZP ceramics. Scripta mater., 43 (2000) 465-470.

78. Shetty D.K., Wright I.G., Stropki J.T., Slurry erosion of WC-Co cermets and ceramics. ASLE Transactions, 28 (1985) 123-133.

79. Wood R.J.K., Mellor B.G., Binfield M.L., Sand erosion performance of detonation gun applied tungsten carbide/cobalt-chromium coatings. Wear, 211 (1997) 70-83.

80. Feng Z., Ball A., The erosion of four materials using seven erodents-towards an understanding. Wear, 233-235 (1999) 674-684.

81. Wang Y-F., Yang Z-G., Finite element model of erosive wear on ductile and brittle materials. Wear 265 (2008) 871-878.

82. Javaheri V., Porter D., KuokkalaV-T., Slurry erosion of steel – Review of tests, mechanisms and materials. Wear, 408-409 (2018) 248-273.

83. Mellali M., Grimaud A., Leger A.C., Fauchais P., Lu J., Alumina grit blasting parameters for surface preparation in the Plasma Spraying Operation. Journal of Thermal Spray Technology, 6 (1992) 217-227.

84. Syamsundar C., Chatterjee D., Kamaraj M., Maiti A.K., Erosion Characteristics of Nanoparticle-Reinforced Polyurethane Coatings on Stainless Steel Substrate. J. Mater. Eng. Perform., 24 (2015) 1391–1405.

85. Shipway P.H., Hutchings I.M., The role of particle properties in the erosion of brittle materials. Wear, 193 (1996) 105-113.

86. Tsai W., Humphrey J.A.C., Cornet I., Levy A.V., Experimental measurement of accelerated erosion in a slurry pot tester. Wear, 68 (1981) 289-303.

87. Levy A.V., The solid particle erosion behavior of steel as a function of microstructure. Wear, 68 (1981) 269–287.

88. Gadhikar A.A., Sharma A., Goel D.B., Sharma C.P., Effect of carbides on erosion resistance of 23-8-N steel. Bull. Mater. Sci., 37 (2014) 315–319.

89. Kumar A., Sharma A., Goel S.K., Effect of heat treatment on microstructure, mechanical properties and erosion resistance of cast 21-4-N nitronic steel. SOJ Mater. Sci. Eng., 4 (2016) 1–5.

90. Meng H.C., Ludema K.C., Wear models and predictive equations: their form and content. Wear, 181-183 (1995) 443-457.

91. Wang G.R., Chu F., Tao S.Y., Jiang L., Zhu H., Optimization design for throttle valve of managed pressure drilling based on CFD erosion simulation and response surface methodology. Wear 338-339 (2015) 114-121.

92. Zhang J., Kang J., Fan J., Gao J., Research on erosion wear of high-pressure pipes during hydraulic fracturing slurry flow. Journal of Loss Prevention in the Process Industries, 43 (2016) 438-448.

93. Singh J., Singh J.P., Singh M., Szala M., Computational analysis of solid particle-erosion produced by bottom ash slurry in 90° elbow. CMES'18, MATEC Web Conf., 252 (2019) 04008**.**

94. Hassan M.A., El-Sharief M.A., Aboul-Kasem A., Ramesh S., Purbolaksono J.,A fuzzy model for evaluation and prediction of slurry erosion of 5127 steels. Materials and Design, 39 (2012) 186-191.

95. Hernik B., Pronobis M., Wejkowski R., Wojnar W., Experimental verification of a CFD model intended for the determination of restitution coefficients used in erosion modelling. WTiUE 2016, E3S Web of Conferences, 13 (2017) 05001.

96. Nicholls J.R., Coatings and hardfacing alloys for corrosion and wear resistance in diesel engines. Mater. Sci. Technol., 10 (1994) 1002–1012.

97. Bhushan B., Fundamentals of Tribology and Bridging the Gab between Macro- and Micro/Nanoscale. B. Bhushan [ed.], Kluwer Academic Publishers, Netherlands, 2014.

98. Carter C.B., Norton M.G., Ceramic Materials. Springer New York, New York, 2013.

99. Preece C.M., Macmilla N.H., Erosion. Ann. Rev. Mater. Sci., 7 (1977) 95–121.

100. Bhandari S., Singh H., Kumar H., Rastogi V., Slurry erosion performance study of detonation gun-sprayed WC-10Co-4Cr coatings on CF8M steel under hydro-accelerated conditions. J. Therm. Spray Technol. 21 (2012) 1054–1064.

101. Quinn T.F.J., The role of wear in the failure of common tribosystems. Wear, 100 (1984) 399–436.

102. Larson J.M., Jenkins L.F., Narasimhan S.L., Belmore J.E., Engine Valves-Design and Material Evolution. J. Eng. Gas Turbines Power 109 (1987) 355-361.

103. Zahavi J., Schmitt G.F., Solid particle erosion of polymeric coatings. Wear, 71 (1981) 191–210.

104. Lima C.R.C., Mojena M.A.R., Della Rovere C.A., de Souza N.F.C., Fals H.D.C., Slurry erosion and corrosion behavior of some engineering polymers applied by low-pressure flame spray. J. Mater. Eng. Perform., 25 (2016) 4911–4918.